Time-programmed release of fluoroscein isocyanate dextran from micro-pattern-designed polymer scrolls

Aleksandr I Egunov, Ayano Inaba, Simon Gree, Jean-Pierre Malval, Katsuhiro Tamura, Yukie Saito, Valeriy A Luchnikov

The manuscript published in Journal of Controlled Release, **2016**, *233*, 39-47.
https://doi.org/10.1016/j.jconrel.2016.05.022

Time-Programmed Release of Fluoroscein Isocyanate Dextran From Micro-Pattern-Designed Polymer Scrolls.

Aleksandr I. Egunov,[1] Ayano Inaba,[2] Simon Gree,[1] Jean-Pierre Malval,[1] Katsuhiro Tamura,[2] Yukie Saito,[3] Valeriy A. Luchnikov[*1]*

[1]Institut de Science des Matériaux de Mulhouse, UMR 7361, CNRS-Université de Haute-Alsace, 15, rue Jean Starcky, Mulhouse 68057, France

[2]Industrial Research Institute of Shizuoka Prefecture, 2078 Makigaya, Aoi-ku, Shizuoka 421-1298, Japan

[3]The University of Tokyo, Department of Global Agricultural Sciences, 1-1-1 Yayoi, Bunkyo-ku, Tokyo 113-8657 Japan

*Corresponding author. Email : valeriy.luchnikov@uha.fr

ABSTRACT In this article we present a relevant strategy for a non-trivial time-programmed release of water-soluble macromolecules from biocompatible μ-containers. The system is based on self-scrolled chitosan acetate (CA) fibers, encapsulated in a poly(dimethylsiloxane) matrix. Mass transfer between a fiber and the external environment takes place via the only opened extremity of the fiber. Fluoroscein isocyanate dextran (FID) is initially deposited at the inner

The manuscript published in Journal of Controlled Release, **2016**, *233*, 39-47.
https://doi.org/10.1016/j.jconrel.2016.05.022

surface of the CA fiber according to a programmed pattern. The FID molecules became mobile after the arriving of the swelling front, which propagates along the fiber's axis upon the immersion of the system in aqueous solution. Diffusion of the macromolecules into the environment is enabled by the open-tube geometry of the swollen part of the fiber, while a programmed kinetics of the drug release is due to patterning of the polymer film prior to rolling. The release of the macromolecules can be retarded by a few hours according to the placement of the FID spot with respect to the fibers orifice. A pulsatile release kinetics is demonstrated for a discrete pattern. A few millimeter spacing of the FID spots results in a few hours time interval between the release impulses. Random walk model is plugged in the effective diffusion coefficient for Fick's law and the release kinetics are simulated.

Keywords: macromolecule; controlled release; model drug; chronopharmacology; chitosan; fluoroscein isocyanate dextran; ATR FTIR spectroscopy.

1. Introduction.

Ever growing knowledge about the molecular mechanisms of disease processes has given rise to a new tendency in the pharmacological science, that is, the design of macromolecular drugs (MDs), which interact precisely via the molecular recognition processes with the required targets and perform in this way the therapeutic intervention. Such peculiarities of the MDs provide them high efficiency and specificity of the therapeutic action. Another modern tendency of the pharmacological research is time-controlled drug administration, recently termed chronopharmaceutics [1-3]. Since human physiology and biochemistry vary during a 24 hour

period according to the so called circadian cycle, some medical conditions are more prevalent at certain periods of the day. For instance, the peak in serum cortisol, aldosterone, testosterone, platelet adhesiveness, or blood viscosity, is observed during the initial hours of daytime. In contrast, insulin, cholesterol, triglycerides, platelet numbers, and uric acid levels, peak later during the day and evening, etc. Therefore, multiple sequences for the administration of a drug, or a combination of two different drugs, at distinctive times, may be beneficial in situations in which not only the amount but also the timing of a dose of drug is important.

Time-controlled administration of the macromolecular drugs is associated with specific problems related to their high molecular weight. The release from polymer matrices, explored with success for low-weight molecular substances, is not optimal in the case of the MDs because of very low diffusion rates the macromolecules in the material. In addition, complete release of macromolecules is limited due to their entanglement within the polymer matrix. In order to optimize the release of the MDs, the drug reservoirs are organized often as hierarchical porous materials, in which the transport of the drug molecules outside the matrix pursues via diffusion along the macropores with diameters of 50 nm and higher. An original approach to produce polymer particles with well-defined micro- and nanochannels was suggested by Liu et al. [4]. The particles are formed by dropping a polymer solution in a less-dense liquid, leading to hydrodynamics formation of toroidal-spiral structure, which is flash-solidified by photo-triggered crosslinking. A macromolecular model drug, polyphosphate, was released by diffusion along the spiral channel in course of a few hours. In another approach, macroporous polymer matrices with the pore sizes of the order of 10-100μm were explored as the macromolecular drug release media, with the release rates determined by the topology of the porous space [5,6].

The manuscript published in Journal of Controlled Release, **2016**, *233*, 39-47.
https://doi.org/10.1016/j.jconrel.2016.05.022

In the present article, we propose a new macromolecular delivery strategy based on elaboration of chitosan-based micro-encapsulation media, which promote the release of the molecules according to a time-programmable kinetics. In our approach, the water-soluble macromolecules are initially encapsulated in biocompatible chitosan acetate (CA) microfibres, which are produced by self-scrolling of differentially strained CA films in aqueous solutions. Arbitrarily complex distributions of the macromolecules concentration along the fiber axis can be realized via 2D-patterning of the films prior to the scrolling step. The fiber is embedded into a water-impermeable matrix in such a way that only one extremity is accessible to the external environment. The kinetics of the release can be controlled by i) the rate of the fiber swelling front propagation starting from the extremity, ii) the distribution of the macromolecules along the fibre's axis, and iii) the mass transport of the macromolecules along the swollen part of the fibre to the extremity. A broad range of the release kinetics can be programmed by taking into account these three factors. In the present paper, we demonstrate the realisation of a pulsatile release profile using fluorescein isocyanate dextran (FID), which is often explored as a macromolecular model drug [7,8].

2. Materials and Methods.

2.1 Preparation of scrollable CA films.

The 1% w.t. solution of chitosan (Sigma-Aldrich, 448877-50g, lot #MKBJ9698V, acetylation degree 20%) was prepared using aqueous solution of acetic acid (1% w.t.) as the solvent. One milliliter of the solution was cast on clean glass slides (7.5 cm × 2.5 cm) and gently dried at 70°C until the formation of the solid film. The average thickness of the films was h=16 μm. The films of the same thickness were obtained also by dip-coating of the glass slides from the 2.5% w.t. solution of CA in the 2.5% w.t. acetic acid, followed by drying at the same conditions. The 63μm

The manuscript published in Journal of Controlled Release, **2016**, *233*, 39-47.
https://doi.org/10.1016/j.jconrel.2016.05.022

thick films were produced by dip coating from the 5% w.t. solution of CA in the 5% w.t. acetic acid. A set of TPP solutions (1%, 2%, 3%, 4%, 6%, and 8% w.t.) was prepared in deionized (DI) water. Acidity of the solutions was adjusted to pH≈3 by adding hydrochloric acid dropwise. Gradient ionic crosslinking of the CA films was achieved by immersing the films for different times in the TPP solution, followed by immediate washing of the samples in DI water and drying with nitrogen stream. The films were rolled by detaching the stripes of the CA film mechanically from the substrate with a doctor blade and then transferring them onto the surface of DI water where the stripes rolled up within a few seconds of contact with water. Rolling experiments should be performed no later than a few hours after the films are prepared, in order to avoid aging effects.

2.2 Loading the CA fibres by FID.

The encapsulation and release experiments were conducted with fluorescein isothiocyanate dextran 500000-conjugate (Sigma Aldrich, 46947, Lot #BCBK4152V). Narrow (0.5mm wide , approx.) stripes of the FID solution were formed on the CA films manually with use of a glass capillary, connected to a syringe. After drying the drug solution, and forming the fibres by self-rolling on the water surface, the dried fibres were encapsulated in polydimetylsiloxane (PDMS) matrix (Sylgard 184 Kit). The ratio of PDMS to the curing agent was 30:1 (instead of the common 10:1 ratio), in order to reduce the stiffness of the matrix and facilitate the opening of pores after the fibers swelling.

2.3 Instrumentation and physical measurements.

Attenuated total reflection Fourier transform infra-red (ATR-FTIR) spectra of the face and the back sides of the films were measured on a Bruker IFS 66/S spectrometer (a diamond ATR cell). Time-dependent experiments for the release of fluorescent dextran have been performed using a FluoroMax-4 spectrofluorometer. The FID-loaded fibres, encapsulated in PDMS matrix, and open

The manuscript published in Journal of Controlled Release, **2016**, *233*, 39-47.
https://doi.org/10.1016/j.jconrel.2016.05.022

at one end by cutting, were introduced into a quartz cuvette that contained 3 ml of water at pH≈9. In this solution, the fibres were positioned on a grid at the upper side of the cuvette to maintain the optical detection window. The cell that was maintained at 25 °C was stirred continuously during the experiment.

2.4 Computer simulation.

The random walk model and the analytical solutions were implemented in the MATLAB R2015a programming environment.

3. Results

3.1 Chitosan acetate self-scrollable films.

Chitosan is a linear polysaccharide, derived by deacetylation reaction from chitin, a naturally abundant biopolymer, which is a characteristic component of cell walls of fungi, and of the exoskeletons of crustaceans and insects. In the chemical nomenclature, chitosan is designated as the random β-(1-4) linked copolymer of D-glucosamine (deacetylated unit) and N-acetyl-D-glucosamine (acetylated unit). Due to their remarkable biocompatibility, antibacterial, antifungal, and hemostatic properties, chitosan and its derivatives are broadly used in medicine and cosmetics [9]. In particular, it is extensively used as the scaffold material of hydrogel drug delivery vessels [10-12].

The manuscript published in Journal of Controlled Release, **2016**, *233*, 39-47.
https://doi.org/10.1016/j.jconrel.2016.05.022

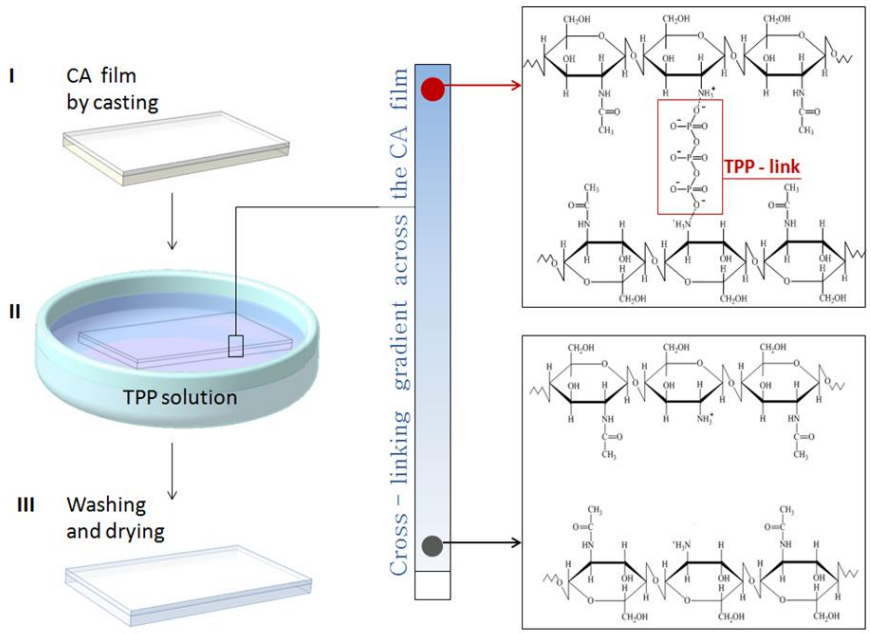

Figure 1. Fabrication of the CA films (scheme). The ionic crosslinking gradient is imparted to the films by their exposure to the TPP solution for a few seconds. The face side of the film, cased on a glass slide, became more densely cross-linked, than the back side, which is adjacent to the slide.

Chitosan is not soluble in neutral water, but became such in acidic aqueous solutions for pH below 6, due to electrostatic charging of the chains via protonation of the amine groups. An aqueous solution of chitosan with acetic acid was used in our research and exhibits good film forming properties. The CA films were produced either by casting, or dip-coating of the CA solutions, as described in the Section 2.1.

As shown in our previous works, in order to impart a homopolymer films the self-scrolling ability in a suitable solvent, one should create the vertical gradient of swelling capacity, with one of the film sides being more swellable than the opposite one [13-17]. For instance, the self-scrolling was observed in the films in which the gradient of the cross-linking density was created [15]. According to the Flory-Renner theory [18,19], the degree of swelling of a polymer network decreases as the crosslinking density increases. The differential swelling generates the gradient

The manuscript published in Journal of Controlled Release, **2016**, *233*, 39-47.
https://doi.org/10.1016/j.jconrel.2016.05.022

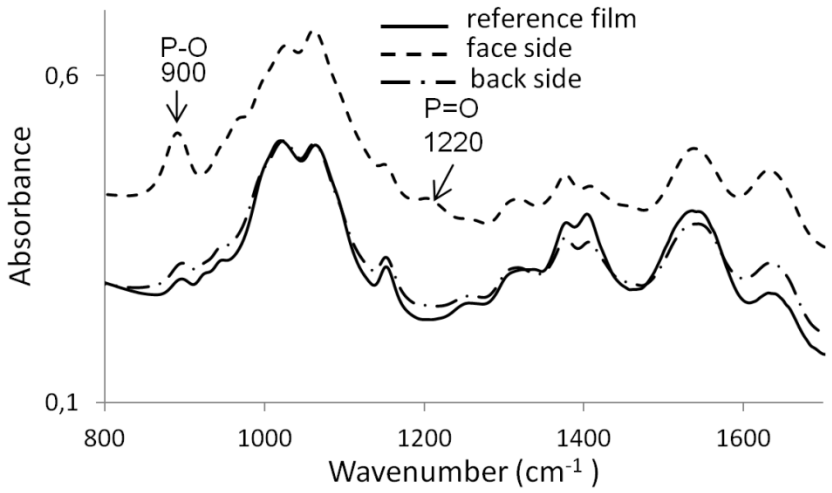

Figure 2. ATR-FTIR spectra of 16μm-thick XA films treated with TPP acidic solution for 3 sec.

of the in-plane stress and the bending moment. If the bending moment is sufficiently strong to overcome adhesion to the surface, or the film is free-standing, the film curls up and forms a tube or a scroll. Chitosan can be covalently crosslinked by glutaraldehyde [20,21], or ionically crosslinked by sodium tripolyphosphate (TPP) [21]. The latter approach is attractive due to non-toxicity of TPP. The TPP-crosslinked chitosan-based hydrogels are stable in basic and slightly acidic (pH>3) water solutions, that makes the TPP ionic crosslinking suitable for our research.

Fabrication of ionically crosslinked CA films is schematically shown on the Fig.1. The TPP bi-anion forms the electrovalent bonds with the $–NH_3^+$ groups of CA, realizing in this way the inter- or intra-chain links. The gradient of the crosslinking density is achieved due to brief (from few seconds to few dozens of seconds, depending on the thickness of the films) immersion of the slides with the CA films into the TPP solution. The gradient of the crosslinking density was confirmed by the attenuated total reflection Fourier transform infra-red (ATR-FTIR) spectra of the face and back sides of the dipped film and the reference spectrum of the fresh untreated film

The manuscript published in Journal of Controlled Release, **2016**, *233*, 39-47.
https://doi.org/10.1016/j.jconrel.2016.05.022

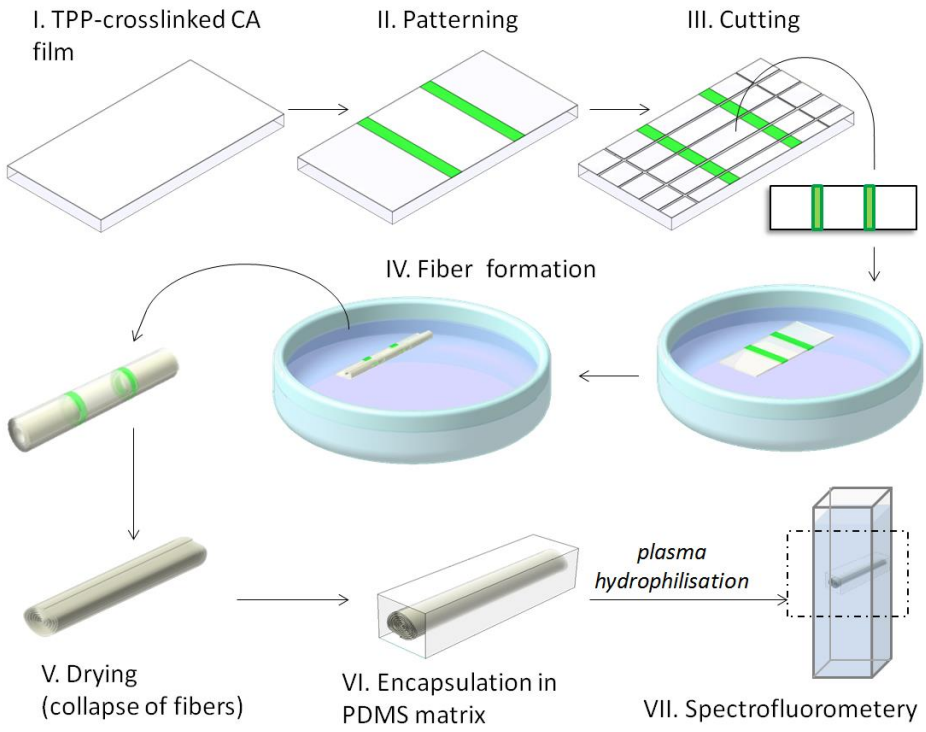

Figure 3. Formation of the fibers, loaded by the model drug, and the drug release experiment (scheme).

(Fig.2). The spectrum of the bottom side resembles that of the untreated reference film. The spectrum of the face side differs significantly from these two spectra due to the clear presence of the P=O and P-O peaks. The brief exposure of the film to the TPP acidic solution therefore forms a vertical structural gradient in the CA films. The time of the film exposure to the TPP solution is important, since the structural gradient can be erased by overexposing the films to the crosslinking solution. The spectra of the face and bottom sides of the film kept in the TPP acidic solution for 1 h approach each other and are characterized by the strong peak that can be attributed to the P=O and P-O groups (Fig.S1, Supplementary Material).

The manuscript published in Journal of Controlled Release, **2016**, *233*, 39-47.
https://doi.org/10.1016/j.jconrel.2016.05.022

3.2 Fabrication of drug patterned µ-fibers.

Fig. 3 depicts the successive processing steps for the fabrication CA µ-fibers which are patterned with FID. Using a syringe filled with an aqueous solution of FID and caped with a very thin glass capillary, the drug patterns are manually drawn at the surface of CA films and consist in one or two parallel FID stripes. The dried CA film is then cut in small pieces, detached from the glass substrate and deposited at the surface of deionized water in such a way that the patterned side does not get in direct contact with water. The tubes which are generated by self-rolling effects after 2-3 seconds in aqueous medium are then extracted and dried at 30°C for a few hours. The tubes drying step induces the complete inner and outer shell collapsing of the structure leading to µ-fibers. Finally, the fiber is embedded in a polydimethylsiloxane (PDMS) matrix in such a manner that only one extremity of the fiber is accessible to the external environment.

The dimensions of the fibers are very sensitive to the experimental conditions. Fig. 4 presents the dependence of the fiber diameter as function of the exposure time of the CA film to the TPP solution (Fig.4a) and as function of the concentration of the solution (Fig.4b). Two thicknesses have been used for the films, $h_1 \approx 16\mu m$ and $h_2 \approx 63\mu m$. For thicker films, the plot of the fibers diameter *vs* the exposure time to the TPP solution exhibits a minimum at 1min, approximately. The existence of this minimum can be explained qualitatively. For a short exposure time, the depth for the penetration of TPP crosslinker within the chitosan film is relatively weak with respect to the film thickness. As a consequence, the superficial crosslinked part of the film hardly counterbalances the overall swelling of the major part of the film which results in a large diameter for the fiber. Increasing the exposure time should lead to the homogenization of the crosslinking density over the film thickness, as pointed above, suppression of the bending

The manuscript published in Journal of Controlled Release, **2016**, *233*, 39-47.
https://doi.org/10.1016/j.jconrel.2016.05.022

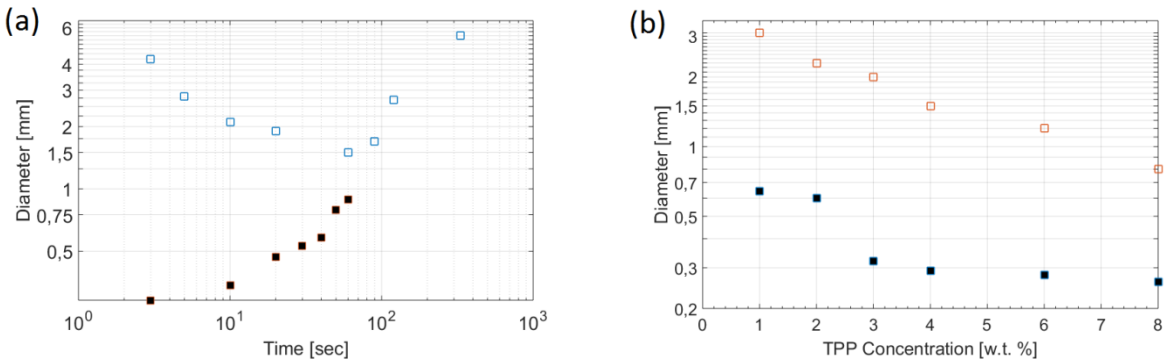

Figure 4. Diameter of the rolled fibres as the function of (a) the time of films treatment in the TPP solution (TPP concentration is w.t. 4%), and (b) the concentration of the TPP solution. *Filled squares:* the film thickness h_1=16 μm. *Open squares:* the film thickness h_2=63μm. For the (b), the treatment time is 10 sec for h_1 and 60 sec for h_2.

moment and, as a consequence, large fiber diameters. This observation is in line with the Timoshenko bilayer beam theory [22], which predicts zero curvature of the beam, either in the case when the thickness of one of the layers aspires to zero with respect to the thickness of the other layer, or in the case of almost identical volumetric response of the layers to an external factor [23]. The minimum of the fiber diameter would exist also for the thinner of the explored films, but it was technically impossible to put the films in contact with the TPP solution for the time shorter than approximately 3 sec. The fiber diameter diminishes monotonously with the TPP concentration for the both film thicknesses (Fig.4b). The time of exposure of the films to the TPP solutions was 10 sec for the thinner films, and 1 min for the thicker ones.

The dependences shown on the Fig.4 were obtained for the outer diameters of the fibers after the self-scrolling step in water (Fig.5). One can distinguish on the optical microscopy images the shells and the cavity in the fibers. The number of the winding is determined by the width of the CA film stripe in the swollen state, and the

The manuscript published in Journal of Controlled Release, **2016**, *233*, 39-47.
https://doi.org/10.1016/j.jconrel.2016.05.022

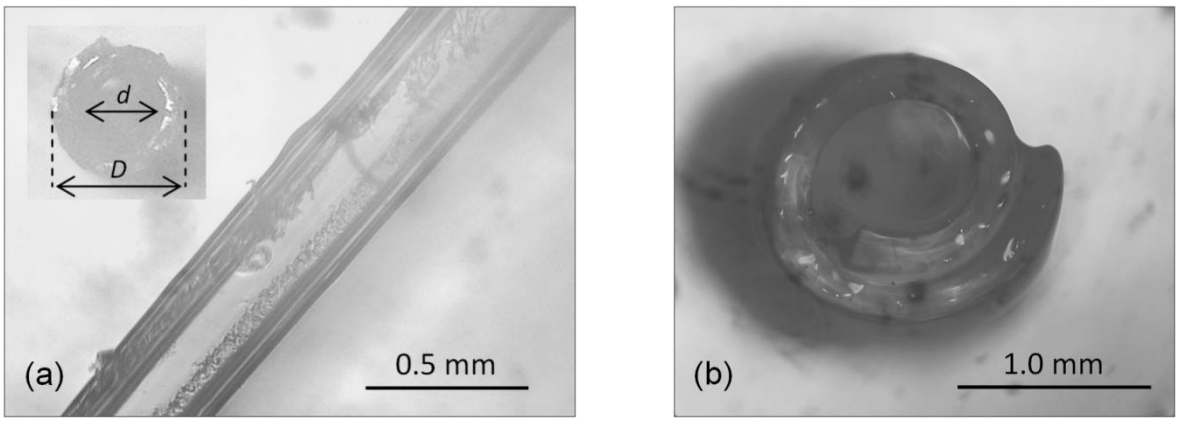

Figure 5. Optical microscopy images of CA fibers, right after the formation in water. (a) A fiber formed by the self-rolling a ≈16μm thick film, after the treatment of the film in TPP solution (w.t. 4%, pH≈3) for 10 sec. *The inset:* the cross-sectional view of the fiber. The inner and the outer diameters are estimated as *d*≈0.24mm and *D*≈0.34mm, respectively. The film thickness in the swollen state is 25μm, approximately. (b) The cross-sectional view of a fiber formed by the self-rolling of a ≈63μm thick film, after the 1min treatment of the film in the same TPP solution. The film thickness in the swollen state is estimated as ≈200μm.

diameter of the fiber. In these present experiments (Fig.4 and Fig.5), the 16μm thick films were typically cut in the 1mm-wide stripes, and the 63μm thick films were prepared as the 2mm-wide stripes. The resulted swelling was by about 210 % and 270 % for thin and thick films, respectively. In this condition, 2 and 1.3 windings were typically observed for the corresponding fibers. It should be noted that larger stripes (approximately 5mm wide) of the 16μm–thick films were used in the macromolecules release experiments presented in the following section. The scrolls formed from these stripes exhibit multiple windings, whose cross-section follows the shape similar to an Archimedean spiral, which reads in polar coordinates $r(\theta) = \frac{d}{2} + \frac{h}{2\pi}\theta$.

The manuscript published in Journal of Controlled Release, **2016**, *233*, 39-47.
https://doi.org/10.1016/j.jconrel.2016.05.022

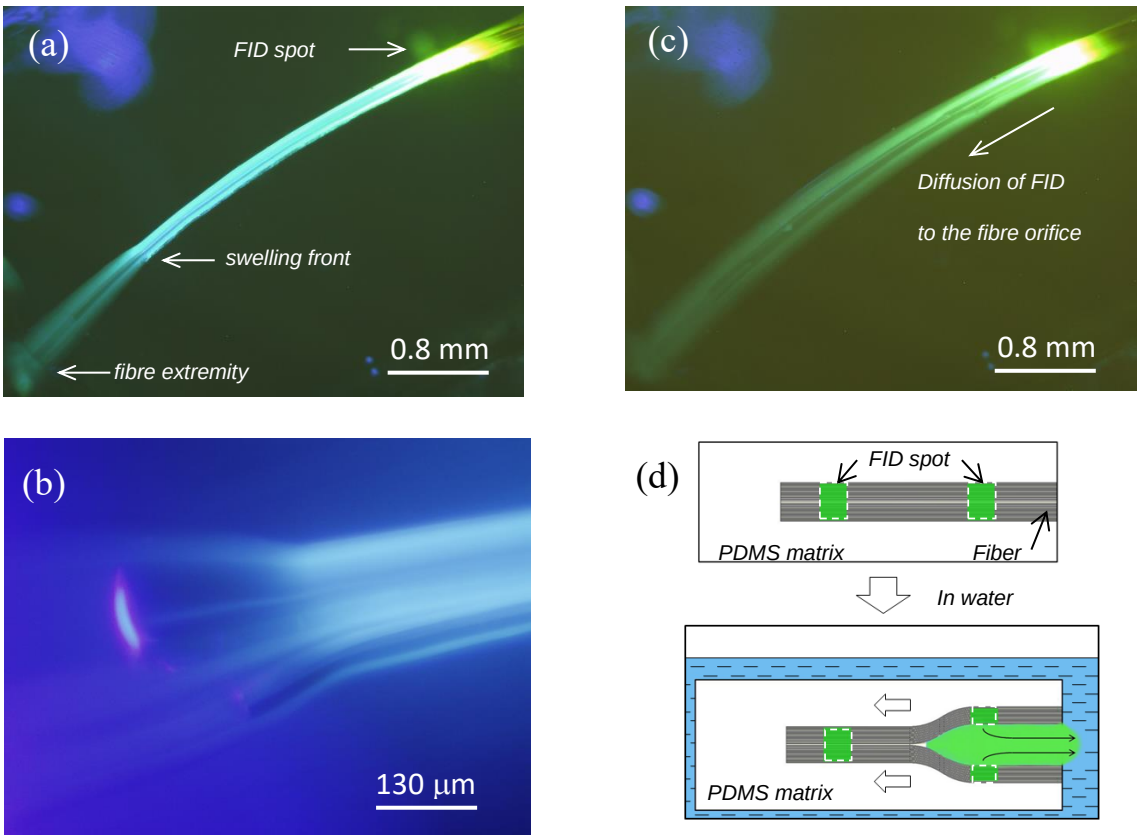

Figure 6. Drug release from the patterned fiber (epifluorescence microscopy). (a) Propagation of the swelling front from the extremity to the inner part of the fiber. (b) Magnified image of the swelling front. (c) Diffusion of FID along the fiber (d) The side view scheme of a patterned fiber, embedded in PDMS matrix, before (top) and after (bottom) insertion in water solution. The open horizontal arrows symbolize the swelling front propagation. The curved narrow arrows indicate the drug escape from the fiber.

It was noted that the inner diameter d diminishes with the number of windings, because the inner windings became squeezed by the outer ones. The comprensive analysis of the shape of the multi-shells fibers requires the energy minimization of the system with respect to the number of winding (or the inner diameter), and will be considered in a special study.

4. Programmed FID release from the patterned fibers.

The µ-fibers were immersed in deionized water and the resulting time-dependent structural changes have been monitored by fluorescence microscopy. Fig. 6a and 6c show two distinctive

The manuscript published in Journal of Controlled Release, **2016**, *233*, 39-47.
https://doi.org/10.1016/j.jconrel.2016.05.022

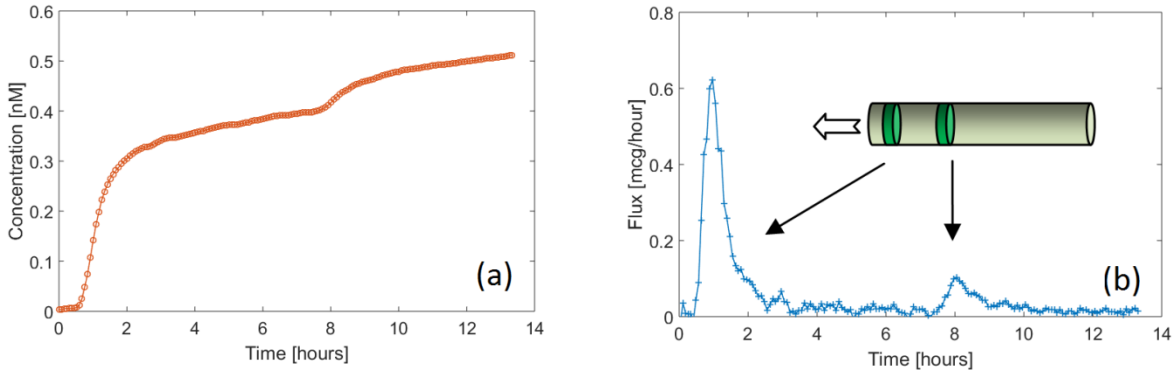

Figure 7 Kinetics of the macromolecules release from a fiber patterned with two FID stripes, positioned at 1mm and 4mm from the fiber extremity, which is in contact with water. (a) FID concentration in water as the function of time. Concentration of FID released from the tube to the aqueous environment has been determined according to a linear calibration curve between the fluorescence intensity of dextran at 511 nm as function of concentration the polymer introduced in the probing aqueous medium as depicted in Fig. S2 of the Supplementary Material. (b) The flux of FID from the fibers extremity.

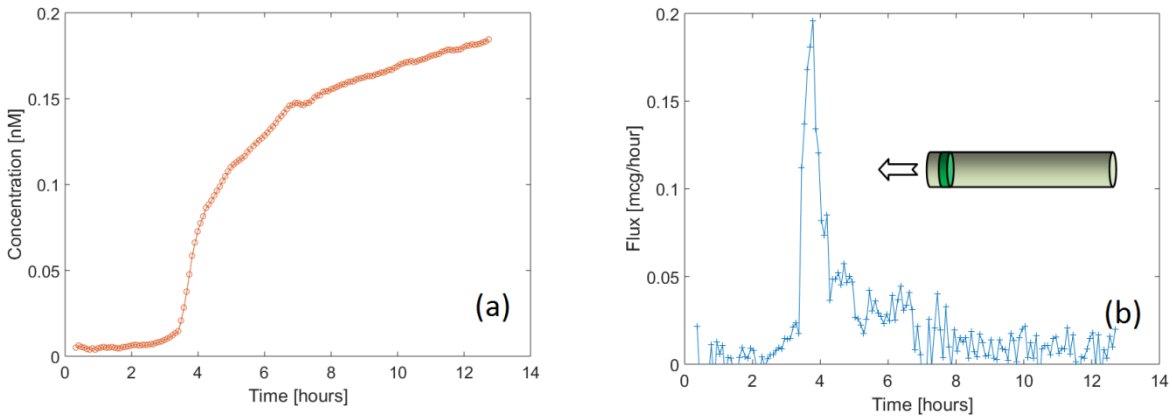

Figure 8 The same as for the Fig.7, for a fiber patterned with one stripe, located at 2.5 mm from the fiber extremity exposed to water. The macromolecules release is retarded by approximately 3.5 hours.

epifluorescence images which has been respectively recorded at initial and final swelling steps of the CA fiber. As shown in Figures 6a and 6b, a swelling front clearly propagates along the fiber

The manuscript published in Journal of Controlled Release, **2016**, *233*, 39-47.
https://doi.org/10.1016/j.jconrel.2016.05.022

axis from the external extremity to inner part of the device. Importantly, encapsuation in the PDMS allows the expansion of the fiber in the direction perpendicular to its axis, due to the low stiffness of the matrix, but inhibits its expansion in the axial direction, so that only a small fraction of the fiber expands out of the PDMS block. The swelling front propagates inside the PDMS block (Fig.6a,b) with the rate of the order of $V = 0.09$ mm/min, decreasing to $V = 0.05$ mm/min in course of 20min of observation. The swelling front becames poorly identifiable as it propagates sufficiently far along the fiber axis. The FID mass transport starts when the swelling front reaches the patterned zone (Fig.6c) allowing the progressive drug dissolution and the subsequent diffusion of FID all along the fiber as illustrated in Fig.6d. Moreover, embedding of the fiber into PDMS matrix implies a one-dimensional mass transport so that the release time-dependent profile of the drug in the external environment should be mainly influenced and modulated by the distance separating the fiber extremity to the FID stripes as well as the distance between the stripes. This provides interesting possibilities for programming the drug release kinetics. Two scenarios have been developed and illustrated by the distinctive kinetics time-profiles displayed in Fig.7 and 8. Fig.7 displays the release time-profile and the FID flux from a μ-fiber in which the first FID stripe is made at $X = 1$mm, and the second stripe is positioned at $X = 4$ mm. The macromolecules release starts approximately 40 minutes after immersion of the μ-fiber in the aqueous medium. A second delivery step is clearly detected at t ≈ 8 hours. The amplitude of the second pulse is several times smaller than the amplitude of the first one. This might be due to diffusional broadening of the pulse, as discussed in the following Section.

The flux curve from the fiber orifice, derived from the concentration time-profile and the known volume of the cuvette, clearly demonstrates the occurrence of two distinctive drug-delivery pulses separated by ≈7 hours. Fig. 8 shows the release kinetics from a μ-fiber with a FID patterning that

consists in a single stripe located at X = 2.5mm from the fiber extremity. The release starts approximately 3.5 hours after immersion of the μ-fiber in the aqueous medium. After this delay, the release time-profile gradually slows down during the 8 hours of observation.

Theoretically, the timing of the pulses is determined by a) the position of the FID stripes in the patterned fiber, b) the rate of swelling front propagation, and c) the rate for the mass transport in the swollen part of the fiber due to convection and diffusion processes. In the absence of any convection phenomena, the characteristic diffusion time from the *i*-th drug spot is estimated as $\theta_i = X_i^2/D$, where X_i is the distance from the spot to the fiber extremity, and D is the diffusion coefficient. The diffusion coefficient of high molecular weight (~500kDalton) dextran in water was estimated as $\approx 8 \cdot 10^{-5} mm^2 s^{-1} = 8 \cdot 10^{-11} m^2 s^{-1}$ [24]. For two FID stripes respectively positioned at X_1 = 1 mm and X_2 = 4 mm, the characteristic diffusion times are about 3.5 hours and 56 hours which are much longer than those measured. Moreover, the experimental times for the macromolecules release do neither correspond to a simple convective time associated to the rate of the swelling front. This means that a non-diffusional mechanism of the mass transfer should play a role in the macromolecules release process from the pore. Possibly, it is related to the flow of water inside the swelling and opening pore. Although the rate of this flow is extremely low, it may provoke local convectional action, due to the imperfections on the walls of the capillary. Air microbubbles entrapped in the dry fiber may be also relevant to the relatively fast escape of the macromolecules from the fiber. More detailed research of the swelling and the mass transfer processes in the fibers is needed for the better understanding of the release mechanisms in the system.

5. Modeling of the FID release kinetics.

The manuscript published in Journal of Controlled Release, **2016**, *233*, 39-47.
https://doi.org/10.1016/j.jconrel.2016.05.022

Programming of a diffusion-controlled drug release kinetics via the nonuniform distribution of the drug in a hygrogel matrix was proposed for the first time in the pioneering works of P.I. Lee [25,26]. In our system, the macromolecules diffuse not through the swollen matrix, but along the tubular marcopore. The comprehensive theoretical description of the drug release from the gradually opening pores should take into account a multitude of the materials characteristics, such as the drug interaction with the pore's walls, possible hydrodynamics effects, mentioned above, and the dependence of the diffusion coefficient on the drug concentration in the solution. In general, the process is highly nonlinear and its predicting would require an elaborated numerical model. Nevertheless, some essential features of the process can be illustrated in frames of a simple theoretical approach and a random-walk model which we propose in this Section. We suppose that drug transport inside the swollen part of the fiber can be represented by the Fick's law, $\vec{j} = -D\nabla C$, where $\vec{j}$ is the flux, C is concentration, and D is an *effective* diffusion coefficient. Assuming that the diffusion takes place essentially along the fibers axis and that the concentration is homogeneous over any cross-section of the fiber, the evolution of the drug concentration in the swollen part of the fiber is described by the linear one-dimensional diffusion equation,

$$\frac{\partial C(x,t)}{\partial t} = D\frac{\partial^2 C(x,t)}{\partial x^2} \tag{1}$$

with the boundary conditions

$$C(0,t) = 0; \qquad \left.\frac{\partial C(x,t)}{\partial x}\right|_{X_S(t)} = 0 \tag{2}$$

The conditions (2) signify the instant dispersion of the drug into the environment from the fiber extremity at $x = 0$, and the absence of the drug transport through the swelling front, situated in the moment t at the coordinate $X_S(t)$. The flux $F(t)$ from the orifice is calculated as

The manuscript published in Journal of Controlled Release, **2016**, *233*, 39-47.
https://doi.org/10.1016/j.jconrel.2016.05.022

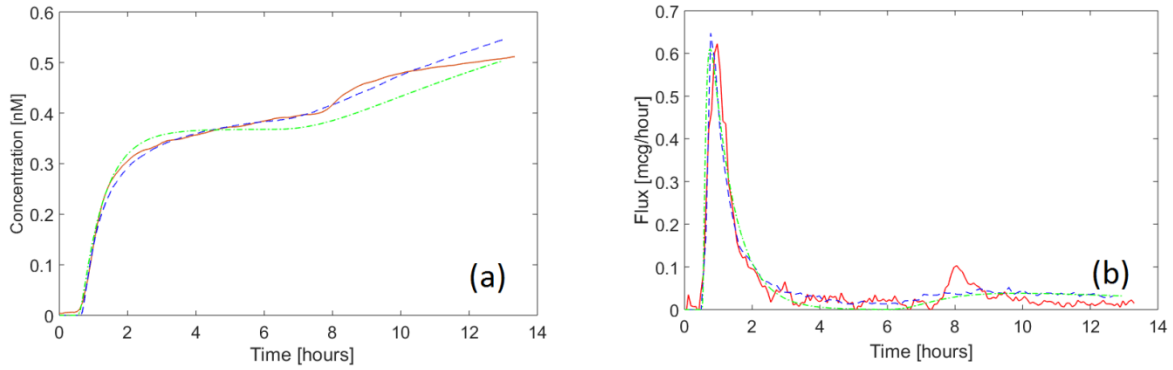

Figure 9. Fitting of the FID release experimental data (solid red lines) presented on the Fig.7 by the random walk model with the moving swelling front (dashed blue line), and by the analytical solution for the quasistationary boundary conditions (dash-dotted green line). The parameters of the RWM: $\Delta t = 0.00014\ hours;\ \Delta x = 0.05mm;$ $p = 0.067;\ \ v_0 = 2.1mm{\cdot}hour^{-1};\ \ X_0 = 2.2mm;$ the initial numbers of walkers at X_1 and X_2 is $N_1 = N_2 =$ 10000, respectively; $f = 5.29 \cdot 10^{-5};\ X_1 = 1mm;\ X_2 = 4mm;\ D = 0.6mm^2hour^{-1} \approx 1.6 \cdot 10^{-10}m^2s^{-1}$. The lag times of the analytical model are $\tau_1 = 0.60\ hour,\ \tau_2 = 5.40\ hours$. (a) The total amount of the released walkers vs FID concentration in the cuvette. (b) The FID flux from the fiber orifice vs the normalized flux of the walkers.

$$F(t) = D\frac{\partial C(x,t)}{\partial x}\Big|_{x=0} \tag{3}$$

In general case, the solution (1) with the nonstationary conditions (2) is not possible in analytical form. In order to address the problem, we consider a random walk model [27]. A fiber is represented by a finite 1-dimensional chain of M sites, with the distance between the sites being Δx. The macromolecules are represented by N "walkers", distributed over the sites. Each walker can jump to a neighboring site (left or right to its current site) with the probability p within the time interval Δt. In the limit $\Delta x \to 0$, $\Delta t \to 0$, $N \to \infty$, $M \to \infty$, the diffusion coefficient in the random walk model (RWM) is $D = \frac{p\Delta x^2}{2\Delta t}$.

The walkers which arrive to the boundary site at $x = 0$, are eliminated from the system and counted. The model was tested by comparison of the calculated flux with the analytical solution

The manuscript published in Journal of Controlled Release, **2016**, *233*, 39-47.
https://doi.org/10.1016/j.jconrel.2016.05.022

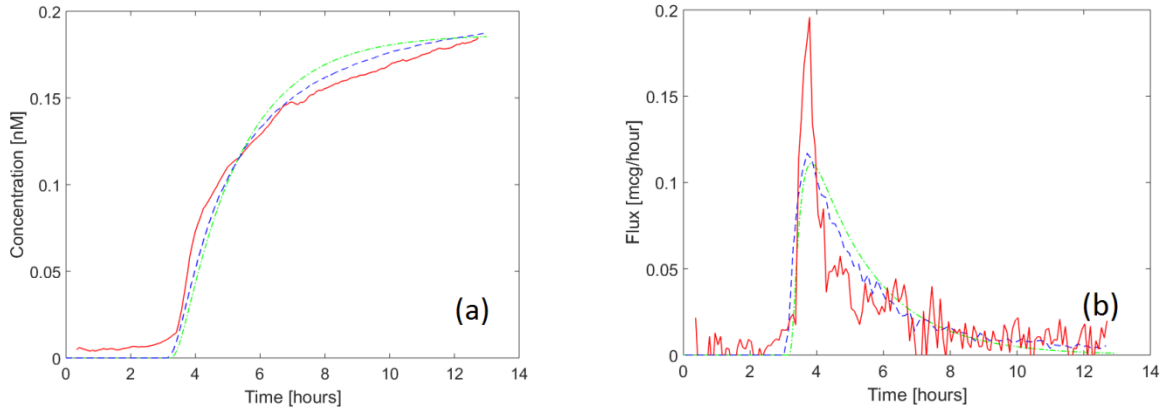

Figure 10. The same as for the Fig.9, for the fiber patterned by a single FID stripe positioned at $X = 2.5mm$ from the orifice (see Fig.8). The parameters of the RWM: $\Delta t = 0.00014\,hour$; $\Delta x = 0.05mm$; $p = 0.15$; $v_0 = 1.1mm{\cdot}hour^{-1}$; $X_0 = 5.0mm$; $N = 10000$; $f = 2.56 \cdot 10^{-5}$; $X = 2.5mm$; $D = 1.34mm^2 hour^{-1} \approx 3.6 \cdot 10^{-10} m^2 s^{-1}$. The lag time of the analytical model is $\tau_1 = 2.94\,hours$.

of (1) for the static boundary conditions $X_S = X = const$ (see the Fig.S3, the associated text in the Supplementary Material, and the Ref.[28]), which reads

$$F_X(t) = \sum_{n=0}^{\infty}(-1)^n \frac{2AD\,\lambda_n}{X} exp\left(-D\lambda_n^2 t\right) \quad (5)$$

Here A is the integral amount of the walkers, $\lambda_n = \frac{(2n+1)\pi}{2X}$, and all the walkers are supposed to be concentrated initially at $x = X$. It is assumed that $F(t) \equiv 0$ for $t \leq 0$. The total amount of the released walkers is

$$\Phi_X(t) = \int_0^t F_X(\tau)\,d\tau = \sum_{n=0}^{\infty}(-1)^n \frac{2A}{X\lambda_n}\left[1 - exp\left(-D\lambda_n^2 t\right)\right] \quad (6)$$

The moving boundary between the swollen and dry parts of the fibers is taken then into account by assuming that the walkers become mobile (can jump to the neighboring sites) if they are positioned left to the current coordinate of the swelling front. Also, the walkers cannot pass from

The manuscript published in Journal of Controlled Release, **2016**, *233*, 39-47.
https://doi.org/10.1016/j.jconrel.2016.05.022

the swollen region to the not swollen one. The coordinate of the swelling front is assumed to be in the form

$$X_S(t) = X_0 ln\left(1 + \frac{v_0 t}{X_0}\right) \quad (7)$$

where v_0 is the initial swelling front propagation rate, and X_0 is a characteristic length, at which the propagation rate slows down by $e = 2.718\ldots$ times. Unfortunately, it was not possible instrumentally to measure the swelling front propagation parameters directly during the fluorometry acquisition. Moreover, the position of the swelling front became poorly identifiable as it penetrates into the PDMS matrix to the depth of 1.5-2mm. Finally, the swelling front propagation may vary from one fiber to another, due to imperfections of their structure. For these reasons, the functional form of the swelling front coordinate (6) only reflects the progressive decrease of the propagation rate, while v_0 and X_0 are the fitting parameters of the model, as well as the diffusion coefficient, and the scaling factor f which relates the number of the released walkers to the concentration of macromolecules.

Fig.9 depicts the the experimental data, obtained for the fiber patterned by 2 FID stripes at $X_1 = 1mm$ and at $X_1 = 4mm$ from the orifice exposed to water basic solution (Fig.7) fitted by the RWM and by the analytical solutions

$$\Phi(t) = \Phi_{X_1}(t - \tau_1) + \Phi_{X_2}(t - \tau_2) \quad (8)$$

$$F(t) = F_{X_1}(t - \tau_1) + F_{X_2}(t - \tau_2) \quad (9)$$

where $\tau_i = \frac{X_i}{v_0}[exp(X_i/X_0) - 1]$ is the time lag corresponding to the time when the swelling front reaches the position of the i-th FID stripe. The diffusion coefficient, and the parameters v_0, X_0, and f of the RWM were defined by iterative process, the least square method being not applicable in this case. The diffusion coefficient of the analytical model is equal to that obtained via the fitting of the experimental data by the RWM. The equations (8), (9) are the superpositions of the solutions

The manuscript published in Journal of Controlled Release, **2016**, *233*, 39-47.
https://doi.org/10.1016/j.jconrel.2016.05.022

of the diffusion equation with the stationary boundary conditions $C(0,t) = 0$, $\left.\frac{\partial C(x,t)}{\partial x}\right|_{X_i} = 0$.

They describe the flux from the fiber without taking into account the finite rate of the swelling front propagation. The experimental data are fitted much better by the solution of the RWM, which incorporates the swelling front propagation rate. It means that the diffusion of the macromolecules in the direction of the swelling propagation (that is, opposite to the fiber orifice) leads to non-negligible effects. Diffusion of the macromolecules over all the swollen part of the fiber seems to be responsible for the slow, but distinctive release between the 2nd and the 7th hours of the experiment, after the first release burst.

Surprisingly, the experimental release rate from the second FID stripe is significantly more intense than the release predicted by the analytical and by the random walk models. Further experiments are needed to elucidate the origin of this discrepancy.

The RWM matches reasonably well the experimental data also for the fiber with the single FID stripe situated at $X = 2.5mm$ from the orifice. As expected, the retarded release is less intense than the kinetic from the spot at $X = 1mm$, observed for the previous experimental system, due to diffusional broadening (see Fig.S4, Supplementary Material). Here again, the finite rate of the swelling front propagation should be taken into account in order to attain the satisfactory fitting of the experimental data by the model.

6. Discussion.

Self-rolled polymer fibers used as water-soluble macromolecules carriers allow achieving time-controlled release kinetics. The release of the macromolecules is enabled by the open geometry of the swollen parts of the fibers, which acquire open tubular geometry after the swelling step. The macromolecules, immobilized initially in a collapsed dry fiber, became then mobile and can freely

diffuse out of the media. Programming of the release kinetics is feasible due to the possibility to create complex distributions of the drug along the fiber axis, via patterning of the polymer films prior to scrolling. Slow rate of swelling front propagation along the axis of the fibers enables good resolution of the release pulses originating from the neighboring spots in the patterned fiber.

The kinetics of the release can be fitted over the period of several hours in frames of the random walk model, which allows to take into account the finite rate of the swelling front propagation from the orifice of the fiber into the depth of the PDMS matrix encapsulating the fiber. Less precisely, the release can be represented by analytical solution of the diffusion equation with the quasi-stationary boundary conditions. The release pulses experience diffusional broadening which is as larger as the the initial materil location is further from the orifice of the fiber. This underlines the difficulty of programming short and intense drug release impulses on large time intervals. The future model should take into account the adsorbtion-desorbtion interaction of the molecules with the inner surface of the fibers. This factor is especially important for the submicron and few micron wide pores because of the high surface to volume ratio for these pores.

The material of the fibers is not limited to chitosan acetate. It can be any biocompatible polymer, to which one can impart the self-scrolling ability. In particular, collagen UV-crosslinked in the presence of riboflavin [29] might be also interesting as a potential material for the preparation of the self-scrollable films for the macromolecular drug encapsulation and controlled release.

The effective diffusion coefficients of FID, found in our fitting study, are approximately two – and sixfold larger than the diffusion coefficient of dextran of comparable molecular mass reported in the Ref.[24]. This is a reasonable difference, taking into account the presumed existence of the convectional flows in the fibers which undergo significant increase of their diameters due to swelling. Yet, the large variation of the diffusion coefficients for the FID release in our system,

and the large discrepancy of the fiber swelling parameters point out on the imperfection of the fibers structure. Further efforts are needed for the unification of the CA fibers characteristics for the truly reliable programming of the therapeutic macromolecules.

7. Conclusion.

In summary, we have developed a new macromolecules release system, capable of the time programming of the release kinetics. In this way, it might be possible to combine two modern trends of the pharmacological research, that is, the chronopharmacology and the use of the macromolecular theurapeutics agents. Our release system consists of the macromolecules-loaded self-rolled chitosan acetate microfibers, embedded in a hydrophobic matrix. Transforming the fibers into tubular macropores upon the swelling step enables the transport of the macromolecules into the environment. Non-trivial time-programmed release kinetics can be achieved via discrete distribution of drug along the fiber axis. Here we demonstrated an original pulsatile time-profile for the drug delivery kinetics. The experimental data are fitted by the random walk model and the analytical solution of the diffusion equation.

Acknowledgements

V.A.L. thanks the financial support by the French National Research Agency, award no. ANR-13-IS09-0002-01.

References

[1] B.-B. C. Youan, Chronopharmaceutics: gimmick or clinically relevant approach to drug delivery? J. Control. Release 98 (2004) 337–353.

[2] P. Wal et al, Chronopharmaceutics as a novel approach for drug delivery. J. Pharm. Sci. Technol. 1 (2) (2009) 59-62.

[3] N. Singh et al, Chronopharmaceutical drug delivery system - a guided therapy. Int. Res J Pharm. App Sci. 3(4) (2013) 84-87.

[4] V. Sharma, M. Szymusiak, H. Shen, L. C. Nitsche, Y. Liu Formation of Polymeric Toroidal-Spiral Particles, Langmuir 28 (2012) 729–735.

[5] W. M. Saltzman, R. Langer, Transport rates of proteins in porous materials with known microgeometry, Biophys. J. 55 (1989) 163-171.

[6] R.A. Siegel, R. Langer, Mechanistic studies of macromolecular drug release from macromorous polymers. II Models for the slow kinetics of drug release. J. Control. Release 14 (1990) 153-167.

[7] D. Horita, M. Yoshimoto, H. Todo, K. Sugibayashi, Analysis of hair follicle penetration of lidocaine and fluorescein isothiocyanate-dextran 4 kDa using hair follicle-plugging method. Drug Dev Ind Pharm (40) 2014 345-351.

[8] Jun Li, Xu Li, Xiping Ni, Xin Wang, Hongzhe Li, Kam W. Leong, Self-assembled supramolecular hydrogels formed by biodegradable PEO–PHB–PEO triblock copolymers and a-cyclodextrin for controlled drug delivery, Biomaterials 27 (2006) 4132–4140.

[9] P. K. Dutta, J. Dutta, V. S. Tripathi, Chitin and chitosan: Chemistry, properties and applications, J. Sci. Ind. Res. 63 (2004) 20-31.

[10] N. Bhattarai, J. Gunn, M. Zhang, Chitosan-based hydrogels for controlled, localized drug delivery, Adv. Drug Deliv. Rev. 62 (2010) 83–99.

[11] P. Roughley, C. Hoemann, E. DesRosiers, F. Mwale, J. Antoniou, M. Alini, The potential of chitosan-based gels containing intervertebral disc cells for nucleus pulposus supplementation, Biomaterials 27 (2006) 388-396.

[12] T.K. Giri, D. Thakur, A. Alexander, H. Badwaik, D.K. Tripathi, Modified chitosan hydrogels as drug delivery and tissue engineering systems: present status and applications. Acta Pharm Sin B. 2 (2012) 439-449.

[13] V. Luchnikov, O. Sydorenko, M. Stamm, Self-Rolled Polymer and Composite Polymer/Metal Micro- and Nanotubes with Patterned Inner Walls. Adv. Mater. 17 (2005) 1177-1182.

[14] V. Luchnikov, L. Ionov, M. Stamm, Self-Rolled Polymer Tubes: Novel Tools for Microfluidics, Microbiology, and Drug-Delivery Systems, Macromol. Rapid Comm. 24 (2011) 1943—1952.

[15] V.A. Luchnikov, Y. Saito, L.A. Tzanis, Novel Fibrous Material Created by Self-Rolling of a Patterned Polymer Thin Film. Macromol. Rapid Comm. 33 (2012) 1404-1408.

[16] L.P Gómez, P. Bollgruen, A.I. Egunov, D. Mager, F. Malloggi, J. G. Korvink, V.A. Luchnikov, Vapour processed self-rolled poly(dimethylsiloxane) microcapillaries form microfluidic devices with engineered inner surface. Lab Chip 13 (2013) 3827-3831.

[17] Y. Saito, V. Luchnikov, A. Inaba, K. Tamura, Self-scrolling ability of differentially acetylated chitosan film. Carbohydr Polym. 30 (2014) 44-48.

[18] P.J. Flory, J. Rehner Jr., Statistical Mechanics of Cross-Linked Polymer Networks II. Swelling J. Chem. Phys. 11 (1943) 521-526 .

[19] P.J. Flory, Statistical Mechanics of Swelling of Network Structures. Chem. Phys. 18, (1950) 108-111.

[20] O.A.C. Monteiro Jr., C. Airoldi, Some studies of crosslinking chitosan–glutaraldehyde interaction in a homogeneous system, Int. J. Biol. Macromolec. 26 (1999) 119–128.

[21] L.-Y. Wang, Y.-H. Gu, Q.-Z. Zhou, G.-H. Ma, Y.-H. Wan, Z.-G. Su, Preparation and characterization of uniform-sized chitosan microspheres containing insulin by membrane emulsification and a two-step solidification process, Colloids Surf B Biointerfaces 50 (2006) 126–135.

[22] S. Timoshenko, Analysis of bi-metal thermostats. J. Opt. Soc. Am. 11 (1925) 233-255.

[23]. The quantitative description of our system in terms of the Timoshenko bilayer theory is not possible, because the CA films are characterized by the continuous gradient of properties in the normal direction to the films.

[24] O. Seksek, J. Biwersi, A.S. Verkman, Translational Diffusion of Macromolecule-sized Solutes in Cytoplasm and Nucleus, The Journal of Cell Biology, 138 (1997) 131–142.

[25] P.I. Lee, Effect of non-uniform initial drug concentration distribution on the kinetics of drug release from glassy hydrogel matrices, Polymer 25 (1984) 973-978.

[26] P.I.Lee, Initial concentration distribution as a mechanism for regulating drug release from diffusion controlled and surface controlled matrix systems, J. Control. Release 4 (1986) 1-7.

[27] G.H. Weiss, Aspects and Applications of the Random Walk, Random Materials and Processes, North-Holland Publishing Co., Amsterdam, 1994.

[28] I. G. Aramanovich, V. I. Levin. Uravneniya matematicheskoy fiziki (in Russian), 2013, ISBN-13: 978-5458265270.

[29] A. Tirella, T. Liberto, A. Ahluwalia, Riboflavin and collagen: New crosslinking methods to tailor the stiffness of hydrogels, Mater. Lett. 74 (2012) 58–61.

The manuscript published in Journal of Controlled Release, **2016**, *233*, 39-47.
https://doi.org/10.1016/j.jconrel.2016.05.022

Supplementary Material

Time-Programmed Release of Fluoroscein Isocyanate Dextran From Micro-Pattern-Designed Polymer Scrolls.

Aleksandr I. Egunov,[1] Ayano Inaba,[2] Simon Gree,[1] Jean-Pierre Malval,[1] Katsuhiro Tamura,[2] Yukie Saito,[3] Valeriy A. Luchnikov[*1]*

[1]Institut de Science des Matériaux de Mulhouse, UMR 7361, CNRS-Université de Haute-Alsace, 15, rue Jean Starcky, Mulhouse 68057, France

[2]Industrial Research Institute of Shizuoka Prefecture, 2078 Makigaya, Aoi-ku, Shizuoka 421-1298, Japan

[3]The University of Tokyo, Department of Global Agricultural Sciences, 1-1-1 Yayoi, Bunkyo-ku, Tokyo 113-8657 Japan

*Corresponding author. Email : valeriy.luchnikov@uha.fr

The manuscript published in Journal of Controlled Release, **2016**, *233*, 39-47.
https://doi.org/10.1016/j.jconrel.2016.05.022

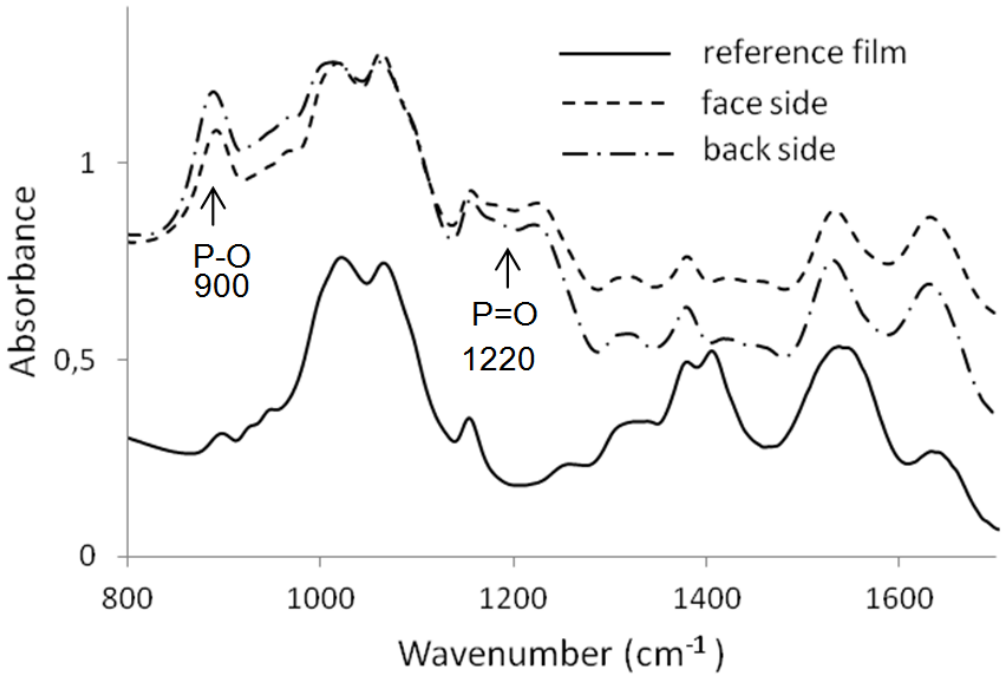

Figure S1. ATR-FTIR spectra of the CA film treated from one side by TPP basic solution for 1 hour, and of the reference (not-treated) film.

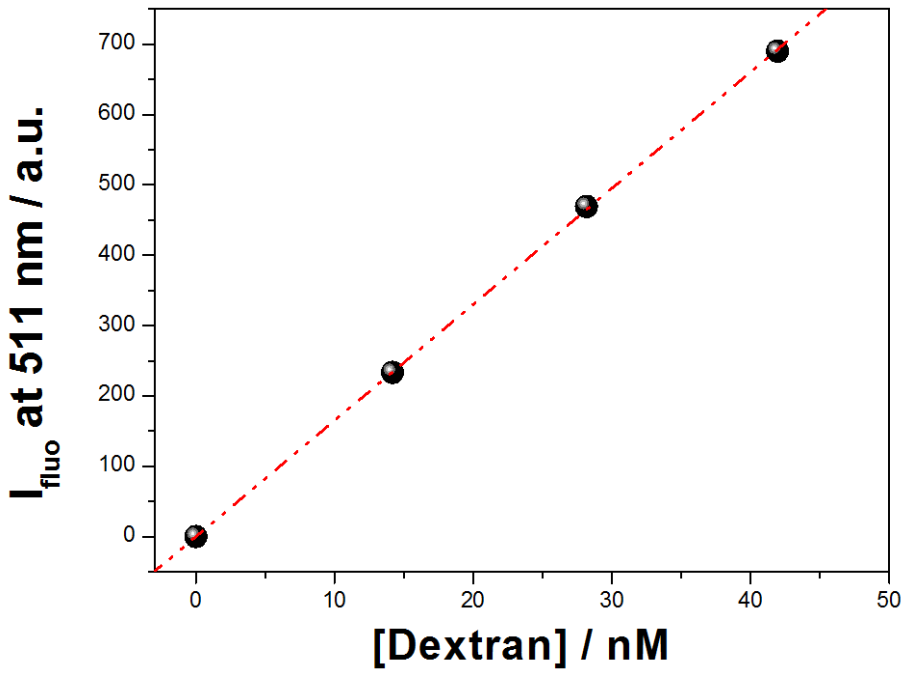

Figure S2. The fluorescence intensity of dextran as function of its concentration in aqueous medium (pH ~ 9)

The manuscript published in Journal of Controlled Release, **2016**, *233*, 39-47.
https://doi.org/10.1016/j.jconrel.2016.05.022

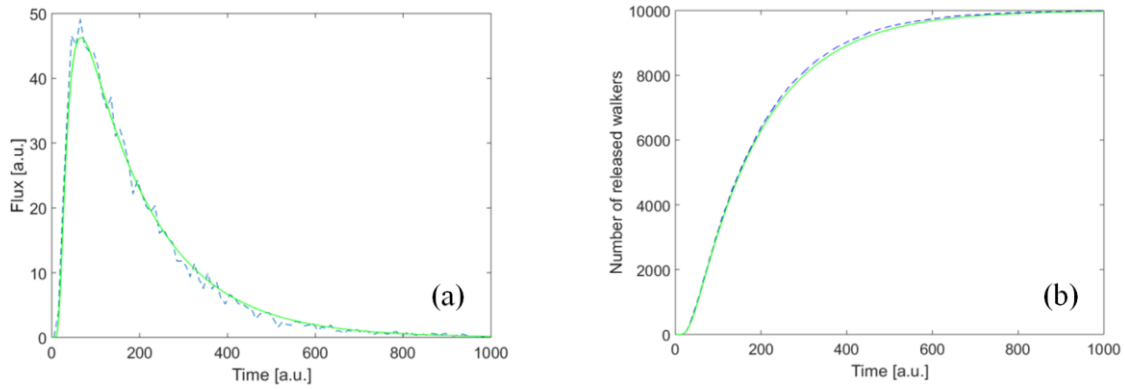

Figure S3. Comparison of the random walk model (dashed blue line) and the analytical solution (solid green line) of the diffusion equation for the stationary boundary conditions. The RWM parameters: M=100; N=10000; $\Delta x = 0.1$; $\Delta t = 0.01$; $p = 0.5$; $D = \frac{p\Delta x^2}{2\Delta t} = 0.25$. At the beginning of simulation, all the walkers are concentrated at the M-th site. The analytical solution parameters: $= M\Delta x = 10$; $D = 0.25$; fifty eigenfunctions of the diffusion equation were taken into account. (a) Flux of the walkers from the linear chain extremity, $F(t)$. (b) Total amount of the walkers, released from the system, $(t) = \int_0^t F(\tau)\, d\tau$.

For the sake of simplicity, we assumed the initial distribution $C_0(x)$ to be pointlike,

$$C_0(x) = A\delta(x - X) \tag{S1}$$

where $\delta(x - X)$ is the Diracs delta-function, and A is the integral amount of the drug in the stripe. The solution of (1) with the boundary conditions (4) and initial distribution (5) reads [25]:

$$C(x,t) = \sum_{n=0}^{\infty}(-1)^n \frac{2A}{X} \sin\ \lambda_n x\, exp\left(-D\lambda_n^2 t\right) \tag{S2}$$

where $\lambda_n = \frac{(2n+1)\pi}{2X}$. Taking the derivative (3) gives the solution for the drug release kinetics from the spot:

$$F_X(t) = \sum_{n=0}^{\infty}(-1)^n \frac{2AD\ \lambda_n}{X} exp\left(-D\lambda_n^2 t\right) \tag{S3}$$

The total amount of the released walkers is

$$\Phi_X(t) = \int_0^t F_X(\tau)\, d\tau = \sum_{n=0}^{\infty}(-1)^{n+1} \frac{2A}{X\lambda_n}\left[exp\left(-D\lambda_n^2 t\right) - 1\right] \tag{S4}$$

The manuscript published in Journal of Controlled Release, **2016**, *233*, 39-47.
https://doi.org/10.1016/j.jconrel.2016.05.022

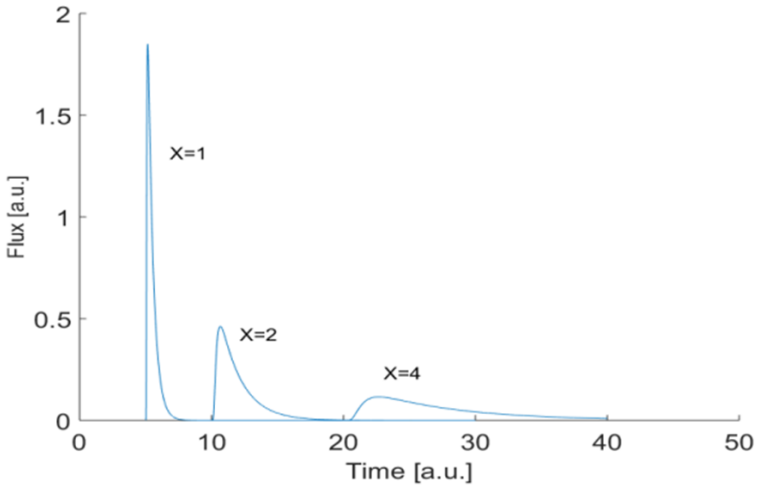

Figure S4. Broadening of the theoretical release kinetics (in arbitrary units) from the material spots positioned at the distances $X_1 = 1, X_2 = 2, X_3 = 4$ from the orifice. The effective diffusion coefficient is $D = 1$.